Effect of Capillary Element Aspect Ratio on the Dynamic Imbibition within Porous Networks[1]

Cathy J. Ridgway[2], Patrick A. C. Gane and Joachim Schoelkopf

Omya AG, CH 4665 Oftringen, Switzerland

ABSTRACT

The Washburn equation is widely accepted for describing capillary imbibition. It has, however, been shown to be insufficient at very short times due partly to the lack of inertial terms. Bosanquet (1) applied an inertial term via momentum, Szekely *et al*. (2), examined single capillaries based on a revised boundary-condition model, and Sorbie *et al*. (3) reviewed and applied Szekely's work to examine the effects of comparative imbibition into a parallel pore-doublet. The study here extends the work of Sorbie *et al*. by applying the equation of Bosanquet to a three-dimensional network model, Pore-Cor. All authors agree that, with the inclusion of inertial terms at short times, smaller radius capillaries will initially fill faster than larger radius capillaries which disagrees with the Washburn equation. It is shown that the aspect ratio of a capillary, defined as its length divided by its radius, plays an important role, in combination with the capillary radii themselves, in determining the filling rate of individual elements. The distribution of this ratio associated with the capillary throat elements within a network structure is investigated. The result is that a preferred pathway of permeation is observed under supersource imbibition conditions in the case where a broad size distribution of capillary elements occurs within a network structure.

Keywords: Imbibition, inertial wetting, imbibition into porous networks, permeation modelling, preferred pathway imbibition, competitive imbibition.

INTRODUCTION

Imbibition of fluids by porous network structures plays an important part in many industrial and environmental applications including oil recovery, water distribution in soil substrates, the manufacture of surface coatings, the application of fluid-based paints and lacquers, and the printing of paper. The long-accepted Lucas-Washburn equation relates the volume rate of fluid uptake by a capillary to the Laplace pressure difference across a meniscus derived from the wetting contact force of the fluid for the capillary wall with a resistive viscous Poiseuille flow simultaneously acting to retard the uptake. This approach has frequently been shown to have shortcomings when considering short timescales especially in pore structures with fine (short) elemental structures, such as might be found in fine sedimentary deposits or in finely structured pigmented coatings (4-15). This is generally considered to be due to the

[1] Running title ' Effect of Capillary Element Aspect Ratio'

[2] Corresponding author, Tel. +41 62 789 2427, Fax +41 62 789 2397, email cathy.ridgway@omya.com

acceleration experienced by a column of fluid entering the capillary or element. Various approaches to the problem have been taken ranging from classical mechanics, including momentum (inertia) (1) and energy conservation (2, 16-20), to molecular dynamics based on individual interactive forces between molecules and between the molecular ensemble and the capillary wall (21). All approaches have various drawbacks. The classical approaches, by definition, cannot accurately describe instantaneous impulse effects without resorting to integrals spanning the initial start of imbibition (1), or there is an unknown energy balance between the imbibing fluid and that within the fluid bulk reservoir (2). The molecular dynamics approaches are as yet limited by computing power and particle number and are not applicable to upscaling in a realistic network model. Furthermore, molecular dynamics are limited by lack of knowledge of the true interactive forces on such a small scale.
A brief review of work carried out in this field allows justification for the choice of approaches which have been further analysed and compared in this paper. One of the earliest approaches to analyse imbibition was reported by Bell and Cameron (22) who found a square-root dependency of time for imbibition which was also found, apparently independently, by Ostwald (23) in 1908. The best-known solution was introduced by Lucas (24) and Washburn (25), which combined the Laplace relation with Poiseuille's equation of laminar flow. The lack of inertial terms, relating to the mass of fluid under motion, was recognised by Rideal (26). Bosanquet (1) complemented Rideal's solution in 1923, adding the inertial impulse drag effect associated with an accelerating fluid.

Bosanquet's publication was effectively forgotten until being uncovered by Wingrave *et al.* (27) in 1978. Szekely *et al.* (2) in 1971 (not referring to Rideal or Bosanquet) started from an energy balance and removed the initial infinity of the Lucas-Washburn velocity. Letelier (17) mentioned that, stripped of arbitrarily added corrective terms, their equation is identical with that of Bosanquet.

Levine *et al.* (16) in 1975 introduced a sink flow towards the capillary entrance from the reservoir, referring to Szekely and adding some changes or improvements. They focussed on the low Reynolds number regime which they considered to be more practically relevant. Levine *et al.* (28) in 1980 account for the deviation from Poiseuille flow in the vicinity of the moving meniscus by including a slip condition. Letelier *et al.* (17) in 1979, (also not referring to Levine's papers) started from the Navier-Stokes equations, discussing both Szekely's and Bosanquet's work. They identified an incorrect coefficient in the second order term, and claimed to have given a more rigorous solution, with dimensionless variables, in the form of a series expansion. Batten (18) in 1984 (not referring to Levine's papers) accepted Letelier's and Szekely's efforts as rigorous but remarked on their disagreement with experimental data. He added to Szekely's equation the dissipation of a kinetic energy head and the initial establishment of a dynamic contact angle. He claimed that the Letelier approach ignored the correction for converging flow at the capillary entry. He compared his own equation, and the two others mentioned, with data from LeGrand and Rense (29). Ichikawa and Satoda (19) in 1993, (not referring to Levine's 1979 work) claimed that Letelier did not account for inertia during the inlet acceleration. They started with an energy balance and arrived at an extended dimensionless Bosanquet relation. Marmur and Cohen (20) in 1997 in turn separated surface tension and radius for individual analysis using an equation for vertical capillarity without specifying the origin. Moshinskii (30) in 1997, only referring to Russian authors,

solved the Navier-Stokes equations using advanced methods to obtain his integro-differential equation. He did not consider the effects at the ends of the liquid column he described. When any of these latter equations are applied to a porous substrate, the number of unknown parameters tends to grow unmanageably.

It is with such a background that the work here is focussed on the following authors. First of all, the initial approach of Lucas (24) and Washburn (25) and then the classical mechanical approaches of Bosanquet (1) and Szekely *et al.* (2), as taken further by Schoelkopf, Gane *et al.* (14, 31) and Sorbie *et al.* (3), respectively, who considered the importance of competitive imbibition into a ratio of different capillary sizes. The competitive rates of imbibition, as manifest by a pore-doublet using the Szekely equation, were shown by Sorbie *et al*. to be related to the aspect ratio of the pores, defined as the length of the capillary representing the pore divided by its radius. These competitive effects in a range of capillaries are compared as modelled by the applications of the Bosanquet equation, the original Szekely equation and a modified Szekely equation derived by Sorbie *et al.* The competitive effect is then introduced and extended to a three-dimensional pore network model[3], using the Bosanquet equation. Various capillary element distributions (throat distributions) are used, each defined by a range of applied capillary aspect ratios, to connect the array of pores, and the wetting permeation is followed through the structure as a function of time.

IMBIBITION KINETICS

Lucas-Washburn

The simplest case for the description of capillarity is represented by a horizontal circular tube of definably small radius, *r*. The Laplace pressure across the meniscus of a fluid in the tube describes the force of imbibition of the capillary and is given by the curvature of the liquid /gas (air) meniscus. To obtain an equation of dynamic motion the Laplace relation is traditionally incorporated into the Poiseuille equation of laminar flow: this was first done by Lucas (24) and Washburn (25) and they obtained the well-known relation

$$x^2 = \left(\frac{rt}{2\eta} \right) \gamma \cos \theta \qquad [1]$$

where x is the distance travelled by the liquid front in the capillary, r is the capillary radius, t is the time, η is the fluid dynamic viscosity, γ is the liquid-vapour interfacial tension and θ the contact angle between the fluid and the solid walls of the capillary.

Momentum and the Bosanquet equation

Bosanquet complemented Rideal's solution (embodying Lucas-Washburn) in 1923 (1) adding the inertial impulse drag effect associated with an accelerating fluid, giving the following force balance:

$$\frac{\mathrm{d}}{\mathrm{d}t}\left(\pi r^2 \rho x \frac{\mathrm{d}x}{\mathrm{d}t} \right) + 8\pi\eta\, x \frac{\mathrm{d}x}{\mathrm{d}t} = P_e\, \pi r^2 + 2\pi r \gamma \cos\theta \qquad [2]$$

[3] Pore-Cor is a software package developed by the Environmental and Fluids Modelling Group of the University of Plymouth, U.K. PL4 8AA.

where ρ is the fluid density and P_e is the external pressure, if applied, at the entrance of the capillary tube.

By integration, and letting

$$a = \frac{8\eta}{\rho r^2} \qquad b = \frac{P_e r + 2\gamma \cos\theta}{\rho r} \qquad [3]$$

it can be shown that

$$x_2^2 - x_1^2 = \frac{2b}{a}\left\{t - \frac{1}{a}\left(1 - e^{-at}\right)\right\} \qquad [4]$$

where x_1 is the initial position and x_2 is the position after time t.

From Eq. [4], it then follows that

$$x_2^2 - x_1^2 \quad = \quad b\,t^2 \qquad (at \ll 1) \qquad [5]$$

If the measurement co-ordinates are set such that x_1 is zero, and there is no applied external pressure P_e, then

$$x^2 = \frac{2\gamma \cos\theta\, t^2}{r\rho} \quad (at \ll 1, P_e = 0) \qquad [6]$$

This equation describes what is referred to as 'inertial flow'. The distance travelled, x, is directly proportional to the time t, in contrast to the Laplace-Poiseuille flow regime described by Lucas-Washburn, Eq. [1], for which x is proportional to $\sqrt{t}$. Also, in contrast, the distance travelled in inertial flow is independent of viscosity, but inversely related to the radius of the element, r, and the fluid density, ρ.

Under the conditions of inertial uptake, the regime of Eq. [6] describes a monolithic block of fluid entering the capillary, driven by the initial wetting force of the liquid contacting the capillary sidewalls. The fluid is assumed to have a flat meniscus front, except in practice at the actual wall contact, and all parts of the fluid within the capillary move at the same rate – hence the independence from viscosity. The flow is retarded more for a high density fluid entering a large capillary because the mass of fluid, and hence its inertia, is higher. Also, the higher the viscosity of the fluid, the faster the effect of viscous drag becomes apparent.

There is a drawback associated with this approach in that the solution to Eq. [2] is undefined at $t = 0$. This can be overcome in practice by applying boundary conditions as limits on the velocity and position which approach zero but do not actually start from zero. This allows for a numerical solution of the equation to be proposed[4].

More satisfactorily, a predictor-corrector method may be used, as described by Ridgway *et al.* (31), applied directly to Eq. [4]. A comparison of the two solutions, evaluated for two capillary radii of 10 μm and 100 μm respectively, shows that they are effectively indistinguishable, Fig. 1, where ρ = 998 kgm^{-3} and η = 0.001 kgm^{-1}s^{-1} apply to the typical case of water as the imbibed fluid. A value of $\gamma\cos\theta$ = 0.2 Nm^{-1} is

[4] Solution obtained from a numerical software analysis package, Maple – a software name of Waterloo Maple Inc., Waterloo, Ontario, Canada N2l 6C2.

used to be consistent with Sorbie *et al.* who, coming from a background of oil/water systems, through replacing oil with air, retain the reduced wetting conditions.

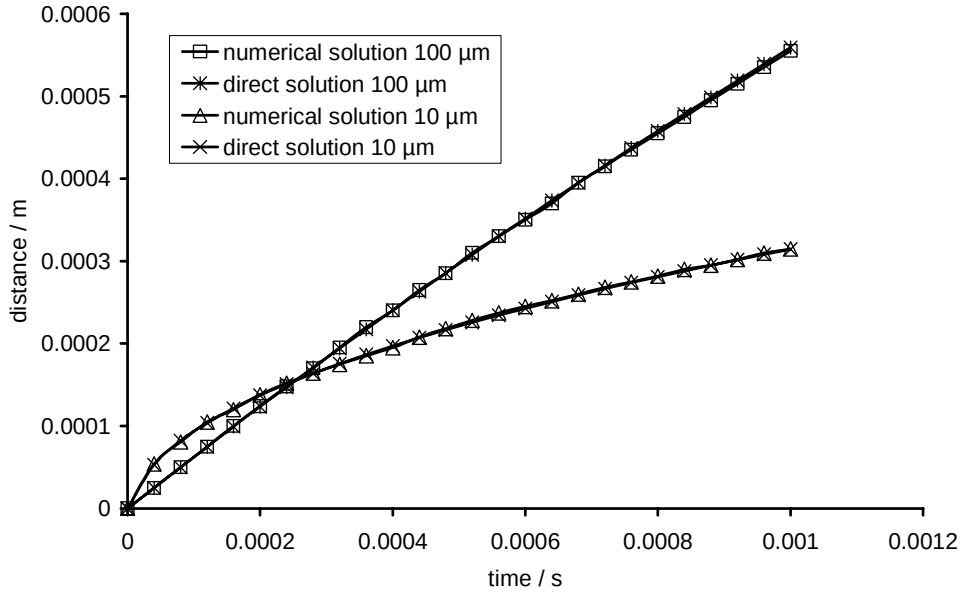

Figure 1. Comparison of two solutions to the Bosanquet equation.

Energy balance and the Szekely equation

Szekely *et al.* (2) also found the Washburn equation to be inadequate at short times. They went on to consider the energy balance at initial fluid uptake and derived the following equation governing the advance of the wetting front in a capillary,

$$\left(x+\frac{7}{6}r\right)\frac{\mathrm{d}^2x}{\mathrm{d}t^2}+1.225\left(\frac{\mathrm{d}x}{\mathrm{d}t}\right)^2+\frac{8\eta}{\rho r^2}x\frac{\mathrm{d}x}{\mathrm{d}t}=\frac{1}{\rho}\left(\frac{2\gamma\cos\theta}{r}-\rho gx\right) \qquad [7]$$

where g is the acceleration due to gravity. The three terms on the left-hand side represent the net influx of kinetic energy, the formation of a vena contracta at the tube inlet and the work expended overcoming viscous forces. The right-hand side consists of a capillary force term and a gravitational potential term, if applicable. Whereas both the Washburn and the Bosanquet approximations are insoluble at $x = 0$ ($t = 0$), predicting infinite velocity, the velocity singularity at $t = 0$ is no longer a problem in the Szekely formulation since the initial conditions, $x = \dot{x} = 0$ at $t = 0$ are computable.

Sorbie *et al.* (3) have shown how this equation compares with that of Washburn by considering water displacing air in a capillary, i.e. external pressure differences are omitted and the effect of gravity over small height differentials is assumed negligible. Sorbie *et al*. also state that the factor of 1.225 in Eq. [7] can be alternatively derived as 0.225.

Comparative solutions to the Washburn, Bosanquet, Szekely and Sorbie equations

The solutions for the two radii of $r_1 = 10$ µm and $r_2 = 100$ µm for the original Szekely equation, the modified version by Sorbie *et al.*, the Washburn equation and the Bosanquet equation are shown in Fig. 2 for the short time range in which the capillaries begin to fill. This graph shows the potential importance of the aspect ratio

(l/r) in that the time taken to fill a short capillary of small radius is shorter than that for a large capillary of equally short length.

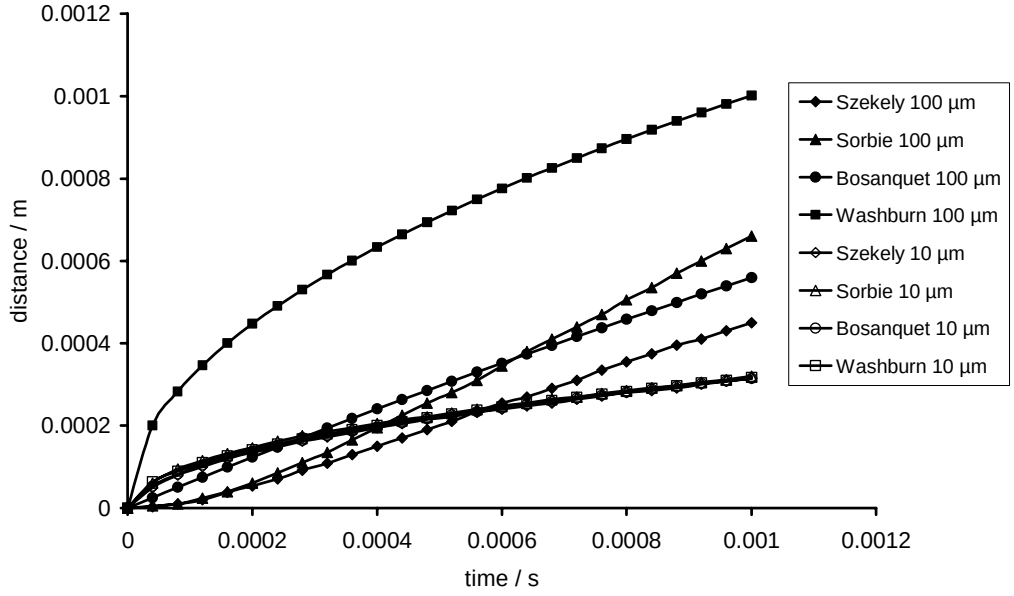

Figure 2. Comparisons of solutions to the equations of Szekely, Sorbie, Bosanquet and Washburn for capillaries of 10 µm and 100 µm.

The four equations give the same imbibition rate for the 10 µm radius capillary. Discrepancies arise for the imbibition behaviour of the larger 100 µm capillary. The solution to the Washburn equation, Eq. [1], indicates that the larger capillary fills at a faster rate at all times. According to this equation, as the capillary size increases so the rate of imbibition will increase, but the fluid density, and thus the fluid's inertia, are not taken into account. The solution to the Szekely equation, Eq. [7], shows the smaller capillary initially filling faster until t = 0.00056 s, when the larger capillary starts to fill at a faster rate. In the larger capillary the density term contributes to inertial retardation, slowing down the imbibition rate at very short times. The two solutions to the Szekely equation (the original and that of Sorbie *et al.*) highlight the effect of changing the constant in the kinetic energy term from 1.225 to 0.225 in Eq. [7]. Initially there is no detectable difference in the rate of imbibition for the larger capillary, but after a short time the imbibition rate increases faster for the smaller value of the constant, and the point where the larger capillary starts to fill faster than the smaller capillary occurs earlier, at t = 0.0004 s. The solution to the Bosanquet equation, Eq. [4], however, may well tend to underestimate the impact of the inertial retardation experienced in the larger capillary. The changeover from the smaller capillary filling faster to the larger capillary filling faster is thus even earlier, at t = 0.00026 s. This is probably because the equation ignores the vena contracta effect incorporated in Szekely. However, it is a point of contention whether a fully developed vena contracta, which can reasonably be argued to exist at the surface entry of a porous medium, can then continue to be manifest between the elements of a network. It is on this basis that the Bosanquet model is pursued in respect to network modelling.

The solutions to the Bosanquet and the Washburn equations were given by Schoelkopf *et al*. (15) for a range of capillary radii and for fluids of different properties. The Bosanquet solution, expressed as a velocity, is shown in Fig. 3, using the fluid properties of water, ρ = 998 kgm^{-3}, γ = 0.07275 Nm^{-1} and η = 0.001 kgm^{-1}s^{-1} and assuming complete wetting, θ = 0. From the diagram it can be seen that on the right-hand side of the maximum velocity ridge, the viscous, Poiseuille, regime applies, while on the left-hand side (towards larger pore radii) the inertial retardation dominates. Therefore, we conclude that there exists a preferred capillary size which evolves as a function of time ranging from the finest, which imbibe with linear *t* inertial wetting at time *t* = 0, up to a given preferred size, after time *t*, defined by the Bosanquet 'ridge' of maximum imbibition.

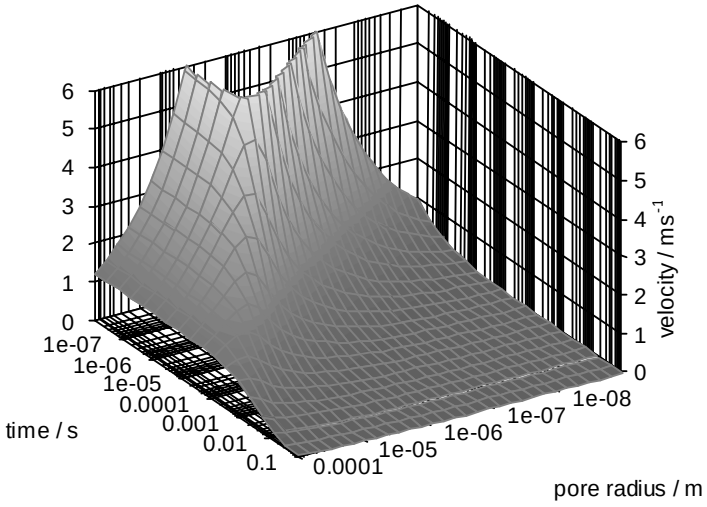

Figure 3. Solution to the equation of Bosanquet as a function of time for a range of capillary radii, expressed as imbibition velocity.

Having shown that capillaries of different dimensions will fill at comparatively different rates, calculated using the Bosanquet equation, Eq. [4], depending on the time of observation, the times taken to fill a range of cylindrical capillaries with varying radii and lengths can be determined. Using a time period up to one second, the shortest times can be expressed as a maximising of the function 1- *t*, Fig. 4. The surface forming the solutions shows that there exist optima distributed over a plane of aspect ratios and radii, such that combinations of these parameters minimise the time taken to fill a capillary of length *l*. Other combinations lying away from this plane become much slower, and when combined in a network will be likely to remain temporarily unfilled in comparison with their neighbours which display more favourable geometries.

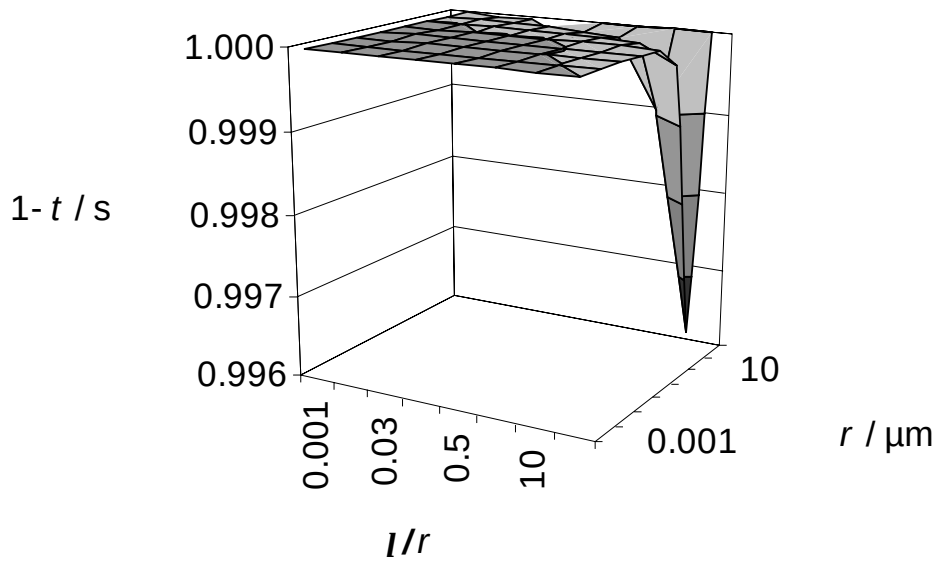

Figure 4. Time taken for water to fill capillaries for a range of capillary radii, *r*, and lengths, *l*, using the equation of Bosanquet.

Thus, we now have the two important controlling components for further analysis, capillary element aspect ratio, *l*/*r*, and the capillary element radius, *r*.

More information about the importance and influence of the *l*/*r* aspect ratio can be seen when the same data are plotted over a range of *l* rather than *r*, Fig. 5.

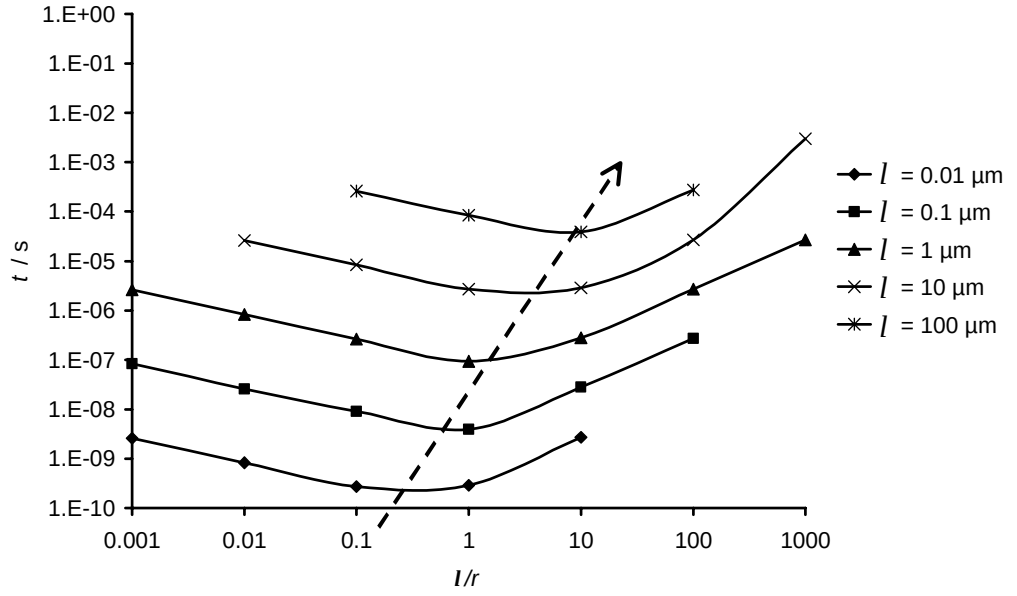

Figure 5. Time to fill capillaries for a range of lengths, *l*, as a function of aspect ratio, *l* /*r*, using the equation of Bosanquet.

The first indication is that for the shortest filling time, t_{min}, over the range of capillary lengths shown in Fig. 5, i.e. for $0.1 < l/r < 10$, $(l/r)_{opt}$, the optimal geometrical aspect ratio for fastest filling, follows an approximate linear dependency (dashed line) given by

$$\log t_{\min} \approx m \log\left(\frac{l}{r}\right)_{\text{opt}} + C \qquad [8]$$

where m and C are constants.

Plotting the above curves as a three-dimensional surface of log$t$ against log(l/r) and log$l$, using the kriging interpolation method adopted in the software package Surfer[5] (geophysical contour method), a surface with an indicative minimum 'valley' is clearly seen, Fig. 6. This graph shows there is a minimum capillary filling time for a specific l/r ratio, $(l/r)_{\text{opt}}$, which is dependent on l.

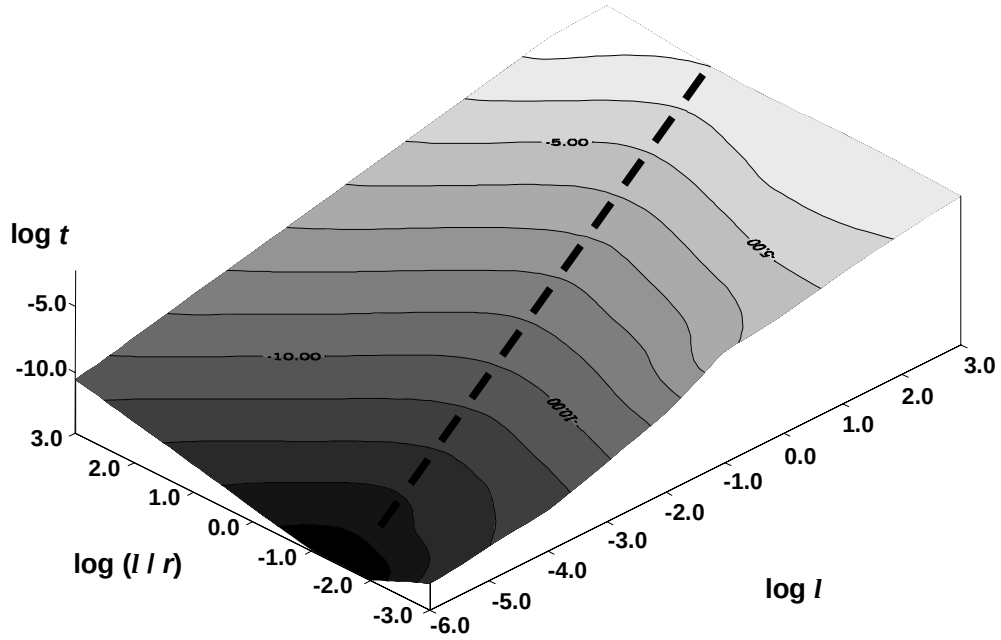

Figure 6. Surface graph for time to fill capillaries for a range of lengths, l, and aspect ratios l /r.

A fit to the three-dimensional surface in Fig. 6 was made using TableCurve 3D[6]. This is shown in Fig. 7, and provides a polynomial equation which can be simplified to the form given in Eq. [9].

$$z = \frac{a + bx + cy + dy^2 + ey^3}{1 + fx + gy + hy^2 + iy^3} \qquad [9]$$

where x = log l, y = log(l/r), z = log t, and a, b, c, d, e, f, g, h, and i are fitting parameters.

[5] Surfer is a software fitting package developed by Golden Software Inc., 809 14th Street, Golden, CO 80401-1866, USA.

[6] TableCurve 3D is a software package developed by SPSS Inc., 444 North Michigan Avenue, Chicago, IL 60611, USA.

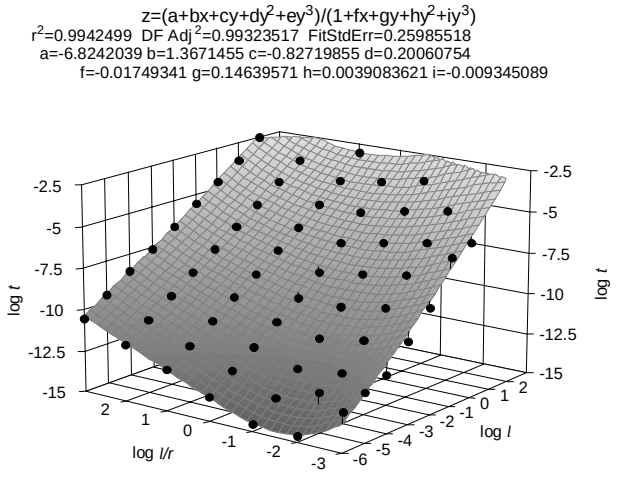

Figure 7. Tablecurve 3D surface fit - the data points are calculated values for water imbibition into capillaries.

The minimum of this surface will be the optimal l/r, $(l/r)_{opt}$, in relation to l for the fastest capillary filling time. For each given capillary length l

$$\log t_{min} = \frac{c + d\log\left(\frac{l}{r}\right)_{opt} + 3e\left\{\log\left(\frac{l}{r}\right)_{opt}\right\}^2}{g + 2h\log\left(\frac{l}{r}\right)_{opt} + 3i\left\{\log\left(\frac{l}{r}\right)_{opt}\right\}^2} \qquad [10]$$

expresses the optimal capillary geometry (aspect ratio) for a minimised filling time. A graphical solution to Eq. [10], using the values derived for the fitting constants in the case of water entering the capillaries, is shown in Fig. 8 on a log/log plot. Over a range of $0.1 < (l/r)_{opt} < 10$, a straight line logarithmic function forms a reasonable approximation, as suggested previously by Eq. [8] above. However, for aspect ratios outside this range the log/log linearity no longer holds.

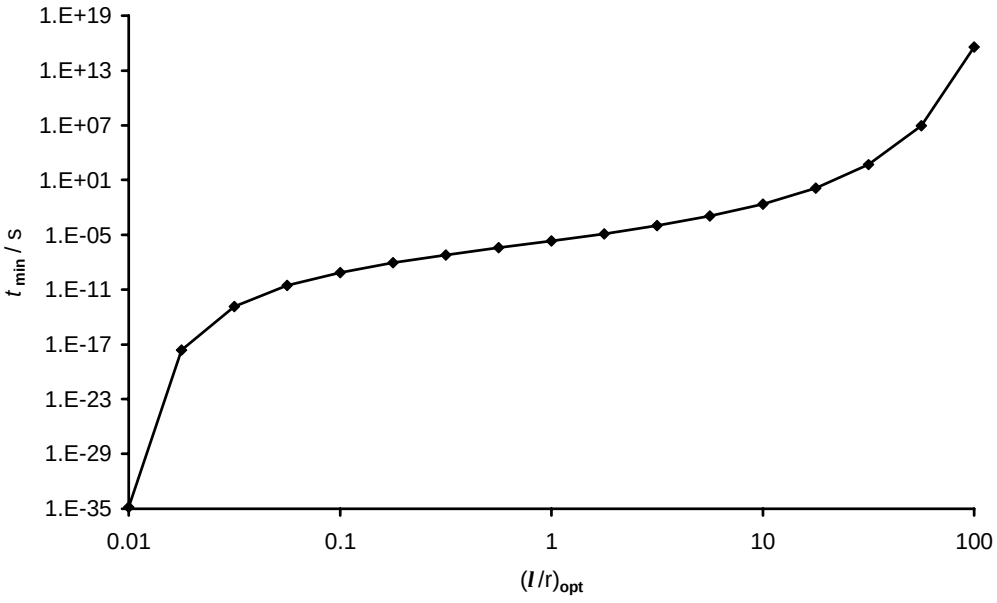

Figure 8. The log/log relationship of minimal imbibition time, t_{min}, for the equivalent optimal aspect ratio $(l/r)_{opt}$ which satisfies eqn [10].

Changes in fluid properties will be further studied in the next section on network structures.

NETWORK STRUCTURES

The network model and the Bosanquet wetting algorithm

Having looked at single capillaries it is important to improve realism in application to interconnected porous structures. Sorbie *et al.* coupled their 'extended Washburn' equation to a formulation of the well-known 'pore-doublet' model based on the development of Chatzis and Dullien (32). They showed that under certain conditions smaller capillaries will fill faster than parallel larger ones. Further work of Sorbie has involved the modelling of two-phase flow in a three-dimensional capillary network and calculating relative permeabilities (33, 34).

In the present work, the Bosanquet equation is applied to the three-dimensional network model[3] and the behaviour of the predicted preferred pathway is demonstrated. The network model simulates the void-space structure of porous materials based on an array of pores and connecting throats. It has been used to simulate the structures of a wide range of porous materials including sandstones, (35), medicinal tablets, (36), and soil, (37) and uses a unit cell consisting of 1 000 cubic pores in a 10x10x10 array, connected by up to 3 000 cylindrical throats, i.e. up to one connected to each cube face depending on the chosen connectivity. The centre of each pore is equally spaced from its neighbouring pores by the 'pore row spacing' Q, and each unit cell is therefore a cube of side length 10 Q. Periodic boundary conditions are applied, i.e. each cell is connected to another identical unit cell in each direction. Connectivity, and therefore flow, is maintained between adjacent unit cells in the x, y, and z directions. When modelling real systems, the pore- and throat-size distribution of the unit cell is optimised so that the simulated percolation curve fits as closely as possible to the corrected experimental mercury intrusion curve (38). The pore and throat size distribution is characterised by two parameters, 'throat skew' and 'pore skew'. The distribution of throat sizes is chosen to be log-linear. The throat skew is the percentage number of throats of the smallest size. The pore size is determined as the size of the largest throat connecting to that pore. The pore skew increases the sizes of the pores by a constant multiple. However, the pores with the largest sizes are truncated back to the size of the largest throat, thus giving a peak at the maximum size. The positions of the pores and throats are random, being determined by a pseudo-random number generator. The percolation characteristics of the network are insensitive to Q. Therefore, after convergence of the simulated percolation to the experimental percolation has been achieved by scanning through values of throat skew and connectivity, Q is adjusted so that the porosity matches the experimental value while ensuring that no pores overlap. It has been found that it is not normally possible to represent the overall complexity of the void network of a natural sample using the relatively simple geometry of a single unit cell. The size of the unit cell is often smaller than the representative elementary volume (REV) of the sample. Therefore, different unit cells must be generated using a different seed for the pseudo-random number generator. The model is designed so that different structural

parameters in conjunction with the same seed of the pseudo-random number generator produce a family of unit cells which are similar to each other – for example, all may have a group of large pores in the same region. This aspect of the modelling is discussed in detail in a recent publication (37). Different stochastic generations use a different pseudo-random number generator seed, and can either use the original optimisation parameters or can be re-optimised to the experimental data. The parameters and procedure are described in detail in previous publications (36, 39).

The Bosanquet equation is used to calculate the wetting flux in each pore and throat in the void network at every time step. To obtain the algorithm for wetting in the network model a reduced form of the equation is defined, which can be compared directly with Eq. [2]. This form was previously applied to a geometry of double conical-shaped throats[7] (31). It is assumed that inertial flow occurs when fluid begins to enter each throat, initially wetting the throat in the form of a monolithic block of fluid as described previously (14, 40). Once a throat is full, the volumetric flow rate of the fluid leaving the throat is calculated and this fluid starts to fill the connected pore. The pore can be filled by fluid from more than one throat, which may start to flow into it at different times. Once a pore is full, or filled to a defined fraction of its volume[8], it starts to fill the throats connected to it that are not already full and which are not already filling from other pores. If at any stage the outflow of a pore exceeds the inflow then a mass conservation restriction is applied which removes this imbalance and restricts the further fluid flow into the network. Mass conservation is used to balance inflow from throats with the outflow dynamic of exiting throats. All throats involved in inflow and outflow are connected to a pore at a node within the model which itself plays no part in the wetting dynamic but acts as a reservoir for onward flow.

At the start of the calculation for wetting into the simulated structure, the total time length for the imbibition is specified. The maximum length of a time step is 1 ns (nanosecond), its value being such that the maximum distance advanced by the fluid in one time step is never more than 0.1 Q. There is also a further restriction on the length of the time step in order to prevent an oscillatory flow behaviour occurring in the throats with very small radii, as explained by Ridgway *et al*. (31). This occurs if $r_{\min}^2 \rho / 4\eta$ is less than 1ns, where $r_{\min}$ is the minimum throat radius in the structure. In this case the time step is set to $r_{\min}^2 \rho / 4\eta$. The flow rate varies greatly with throat diameter, with the consequence that many millions of timesteps must be calculated.

[7] The simulations here use throats consisting of constant radii capillaries.
[8] This work adopts a completely filled pore criterion.

Position of fluid front in a network: defines a preferred pathway with range of r and l/r

To illustrate the controlling effect identified above for single capillaries of the two parameters pore radius, r, and pore aspect ratio, l/r, within a three-dimensional network, two artificial structures were generated with all the throats being kept at a given length in each case, l = 0.03 μm and 1.51 μm, respectively. The different throat lengths were generated by using porosities of 95 % and 20 % respectively. The pore size distribution was monosize. The range of throat radii in both structures was made to consist of 100 sizes spread linearly on a log scale from 0.001 to 1 μm, and the unit cell pore structures were given a connectivity of 4. This size range is applicable to paper coatings where the authors' research interests lie. Water was used as the simulation fluid (ρ = 998 kgm^{-3}, γ= 0.07275 Nm^{-1}, θ = 0 and η = 0.001 kgm^{-1}s^{-1}) and the wetting front was tracked through the unit cell as the fluid front advanced. It is possible to observe exactly the size, and hence the l/r aspect ratio, of the throats which are filled at each given timescale. This procedure allows the distribution of throats which are involved in preferred pathway filling to be identified.

Firstly, the unit cell for the shorter throat lengths is shown in Fig. 9. Clearly, the structure shows little separation of the cubic pores and much of the wetting through the short throats is therefore expected to be inertial.

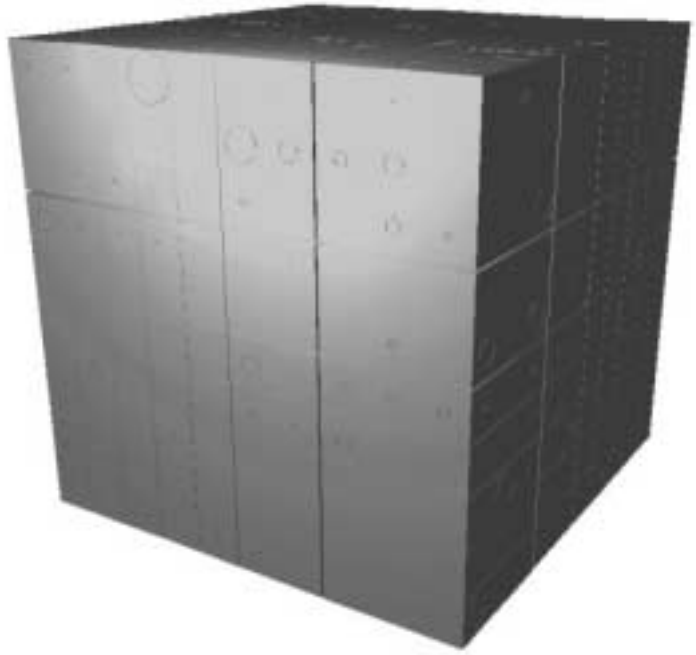

Figure 9. Network model unit cell with throat length, l, of 0.03 μm.

The first layer of throats in the unit cell fills, as expected, as a function of l/r, Fig. 10. This first layer of throats acts as a bundle of single non-connected capillaries: connectivity only being encountered at the first layer of pores connected with these throats. The distribution of l/r is shown on the x axis and the proportion of each throat filled after 0.0009 μs is shown on the y axis. It is clear that the optimum aspect ratio for filling these 0.03 μm long capillaries is $(l/r)_{opt}$ = 0.5.

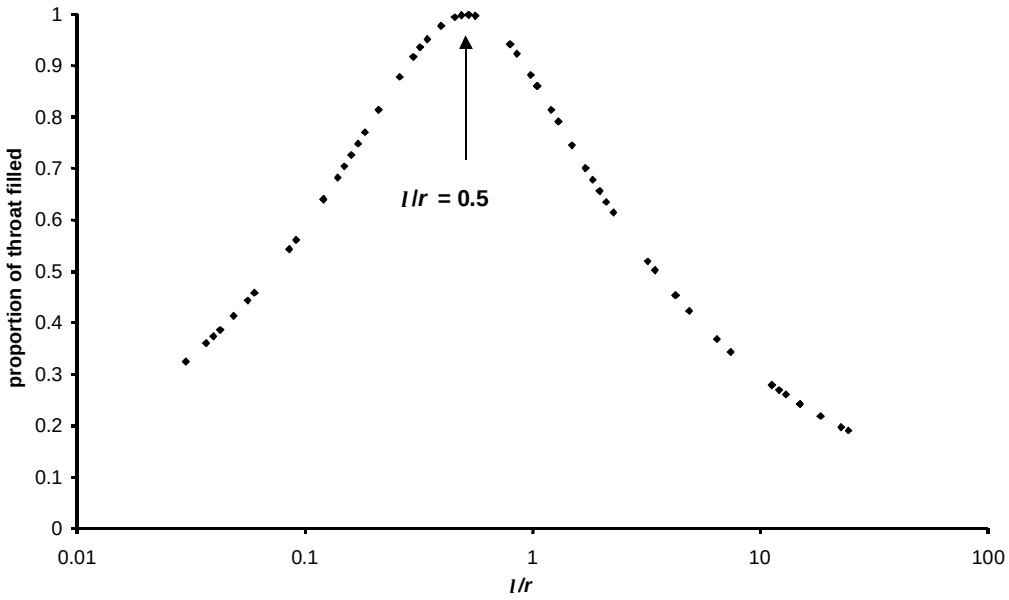

Figure 10. For top layer of throats (single capillaries), the proportion of each throat filled after 0.0009 μs shows an optimum $(l/r)_{opt}$ ratio of 0.5.

The position of the fluid front progressing through the subsequent connected pore network structure at different times can be followed (Fig. 10). After an imbibition time of 0.001 μs the throats which are full have a ratio of l/r between 0.8 and 0.3. At 0.005 μs throats of both larger and smaller radii have now become filled, this range is extended further by an imbibition time of 0.01 μs. At an even later imbibition time of 0.5 μs, two identifiable throats in the second layer of the unit cell are starting to fill from the pores fed from the first set of interconnecting throats. These two throats have l/r ratios of 1.2 and 0.5, respectively. By 2 μs throats with ratios larger and smaller than these are filled. The third layer has three filled throats after 5 μs. These three filled throats have l/r values of 2, 1.4 and 0.2. After 20 μs, the fourth layer starts to fill at a point where the aspect ratio is 0.6, and after 500 μs the fifth layer has a throat full with an aspect ratio of 0.17, and so on. It becomes clear that the first throats in each layer to fill have an aspect ratio of $l/r \sim 0.5$. This is clearly a radius selective mechanism in this structure of constant length throats as the full range of possible values of l/r within this unit cell spans three orders of magnitude (0.03 - 30). Forward imbibition from a filled pore undergoes the effective throat selection imposed by the rate defined under the Bosanquet algorithm and under the constraints of mass balance. In the given structure, after 10 μs, the number of pores emptying whilst under the restrictive mass balance constraint are 23 compared with 22 pores emptying without the need for application of the constraint, i.e. ~ 50 % of pores have an exit dynamic slower than their filling dynamic and the other ~ 50% empty at the same rate as they filled. This illustrates how the combination of the mass balance and the preferred pathway give a distribution of forward filling.

Secondly, the unit cell with the same size range and distribution of features but with longer throats, l = 1.51 μm, and smaller porosity, 20 %, is generated, Fig. 11. In this case, the monosize cubic pores are significantly separated by the longer throats.

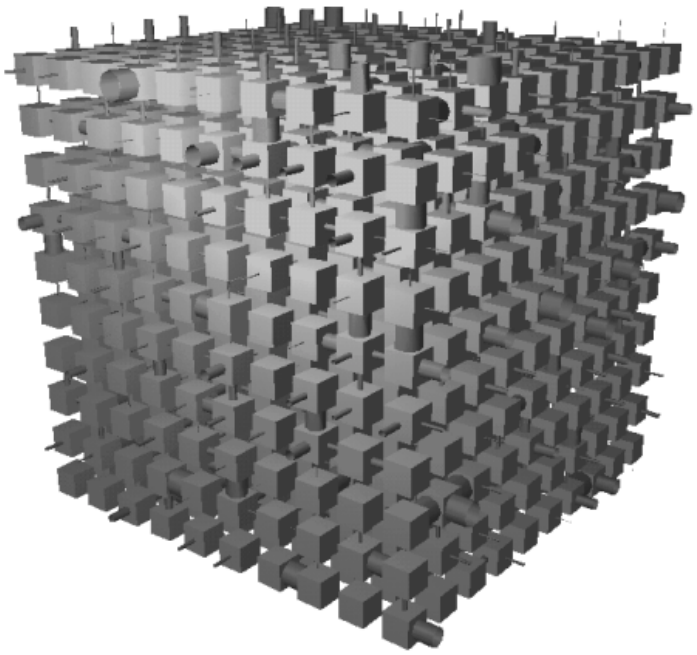

Figure 11. Network model unit cell with throat length, *l*, of 1.51 µm.

The simulated imbibition of water into this structure is similarly analysed as before noting the number and position of filled throats as a function of time.

The full range of *l*/*r* in this case again spans three orders of magnitude (1.51 – 1 510). After 1 µs there are already a number of full throats, all at the smallest *l*/*r* aspect ratios. As the imbibition time increases, throats with progressively larger ratios in the first layer are filled. After 10 µs the second layer of throats is starting to fill, these throats have aspect ratios between 173 and 23, and after 20 µs smaller aspect ratio throats are starting to fill. At 50 µs, the third layer contains filled throats of ratios 99 and 70, and at 100 µs the smaller throat, of aspect ratio 1.51, has finally filled. In this structure, after 100 µs, the number of pores emptying whilst under the restrictive mass balance constraint are 18 compared with 20 pores emptying without the need for application of the constraint, so again ~ 50 % of pores have an exit dynamic slower than their filling dynamic and the other ~ 50% empty at the same rate as they filled illustrating how the combination of the mass balance and the preferred pathway give a distribution of forward filling.

From the previous analysis using short throats, it was seen that a value of $(l/r)_{opt} \sim 0.5$ is optimal for the fastest filling of cylindrical throats by water. For the longer throats, however, the ratio range starts above this value. However, it is clear that the lower aspect ratio throats fill first and that the ones with aspect ratio much larger than 0.5 fill afterwards. Universally, therefore, the optimal void feature aspect ratio for these fluid properties tends toward 0.5, and those features with aspect ratios lying closest to 0.5 in a network structure will fill first provided they are small enough in radius to include the inertial wetting regime, and irrespective of resistive mass balance restrictions.

Increasing the density, viscosity and contact angle of the fluid

The effect of increasing either the density or the viscosity of the fluid used in the imbibition simulation is now studied.

The effect of increasing the density of the fluid by a factor of 10 in the network structure with short throats, whilst keeping the viscosity constant (η = 0.001 $kgm^{-1}s^{-1}$), was investigated. The first throats to fill in the subsequent layers after the initial layer still have $(l/r)_{opt} \sim 0.5$. The time taken, however, to fill the same proportion of unit cell has doubled compared with the lower density simulation.

The effect of increasing the viscosity by three orders of magnitude in the structure with short throats is that the value of $(l/r)_{opt}$ is initially smaller for the first layer, but from there on the ratio tends again toward ~ 0.5. The time taken to fill the structure is the same as for the lower viscosity simulation indicating the dominance of the inertial wetting regime in a structure of extremely short length features which is largely independent of viscosity. In the case of a structure with longer throats, however, the time taken to fill the voids increases significantly as a function of viscosity on account of the viscous drag in the longer capillary elements (41).

Increasing the contact angle, but maintaining the viscosity and density of water slows down the imbibition rate but does not affect the filling pathway, i.e. it has no effect on the value of $(l/r)_{opt}$.

Large versus small range of network feature sizes (radii and (l/r) aspect ratios).

In real structures there will be a range of both throat radii and of throat lengths giving a distribution of aspect ratio over the range of radii. To simulate this further step to reality, the network model has been used to generate two structures with different throat radii ranges, one to represent a coarse structure and one to represent a fine structure. The two structures used to exemplify this were generated with throat radii of 0.05 - 2.50 μm and 0.001 - 0.050 μm, respectively, distributed evenly over a logarithmic scale. The throat length ranges in these unit cells are 0.504 – 5.290 μm and 0.000221 – 0.095900 μm respectively. By careful choice of unit cell sizing, the two structures were selected to have similar resultant porosities, each of ~ 30 %. The pore and throat size distribution for the larger size range is shown in Fig. 12. In the generation an equal number of all the throat sizes is used, however there is an increasing number of pores as the pore size itself increases. The pore sizes are determined by the diameter of the largest throat entering them, as previously stated, and are generated in the unit cell by randomly positioning the throats within the 10x10x10 network. This results in a throat length distribution for the pore and throat size distribution in Fig. 12 as shown in Fig. 13. It is seen that there are only a small number of the longest throats. For a long throat to exist, it must be connecting two small pores. In turn, for a small pore to be generated there must only be throats with the smallest radii leading to it. As the throats are randomly positioned within the unit cell this double constraint makes the probability that all possible throat sites around the two pores will have the smallest radii throats extremely low, hence the low occurrence of long throats. For example, just one large throat in the vicinity will generate a larger pore and thus result in a shorter throat length.

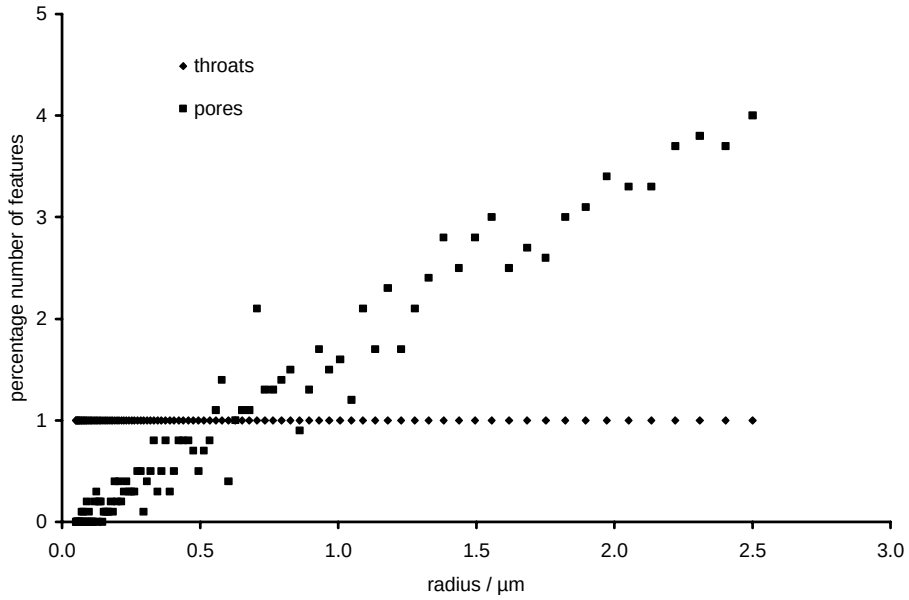

Figure 12. Pore and throat size distribution for structure generated with throat radii of 0.05 - 2.50 µm.

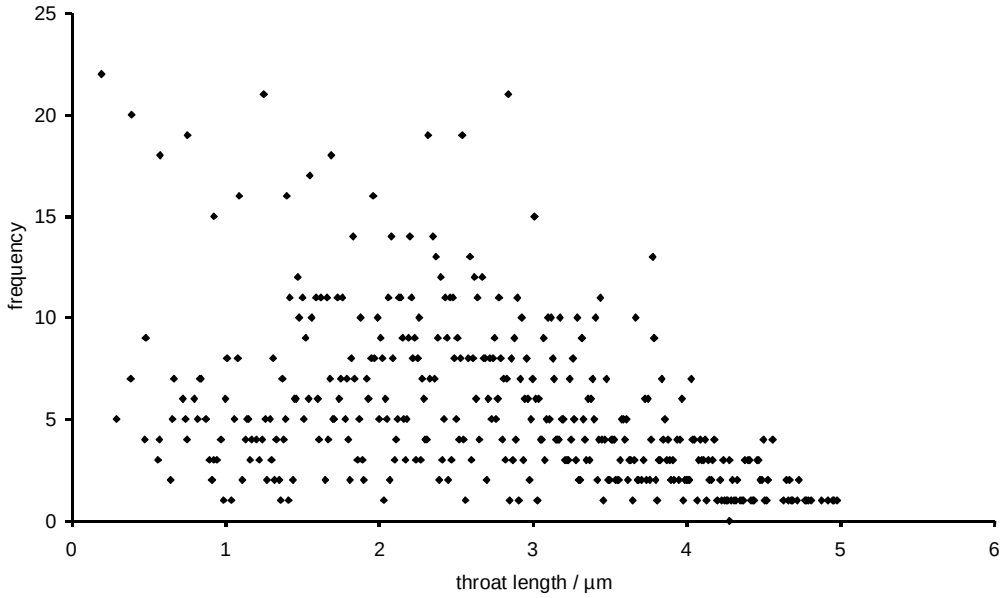

Figure 13. Throat length distribution for structure generated with throat radii of 0.05 - 2.50 µm.

The structures, therefore, have a wide range of pore size, throat radius and throat length, i.e. all the important features discussed previously.

It is seen in Fig. 14 that the rate of imbibition into these more realistic structures, expressed as volume of fluid absorbed per unit area of the sample cross-section, *V*/*A*, at the shortest times favours the finer structure, whereas at larger times it favours the coarser structure, despite both structures having similar porosity. This is similar to the single capillary behaviour predicted by inertial wetting shown previously in Fig. 1. The cross-over point for water as the imbibing fluid occurs at $t = 1.8 \times 10^{-8}$ s. This

also corresponds with accepted reality, and confirms the importance of considering inertial wetting within a network structure on account of the short duration times involved in filling short connecting features. For example, in the case of offset ink tackification and setting, the initial tack increase is controlled by the fine pores in a coating structure, and the progression to setting over longer times is a combined function of the remaining retained capillarity and the unfilled porosity resulting in a total void volume of the coating as permeated by the fluid phase of the ink (42).

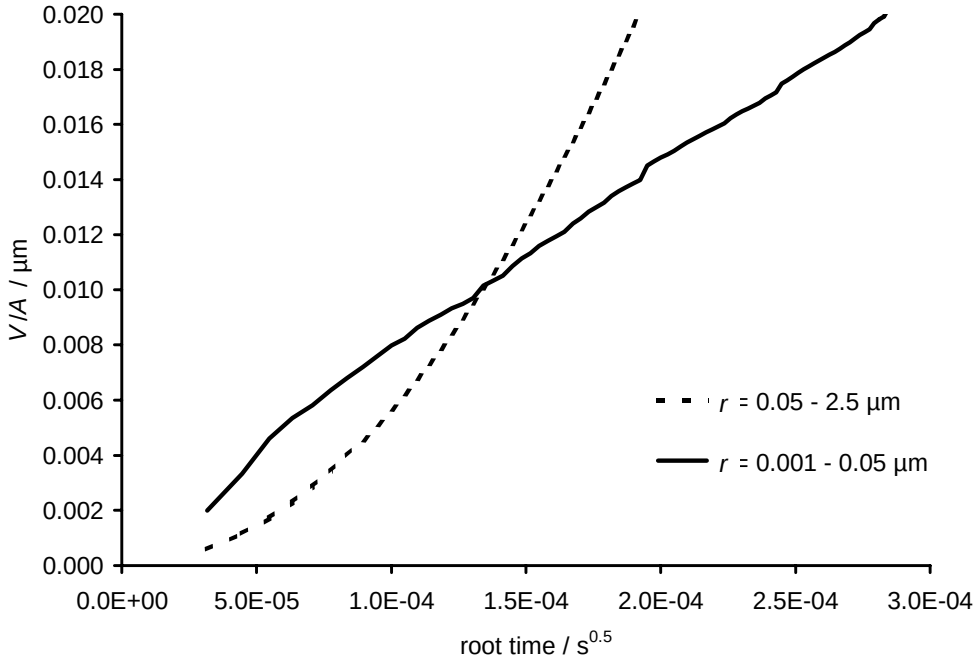

Figure 14. Short-time imbibition into a network structure for coarse and fine broad pore and throat size distributions at similar porosity, expressed as volume absorbed per unit area of contact between substrate and fluid supersource.

SUMMARY

Various classical mechanical models of fluid imbibition into single capillaries have been compared. The need to include inertial wetting terms when considering a network pore structure consisting of microscopic features has been emphasised, and the application of inertial wetting is extended beyond the traditional pore-doublet. The equation of Bosanquet has been used to study the dynamic of fluid imbibition into a porous network structure using a computer model and is shown to predict a preferred pathway of imbibition that is defined by an optimal aspect ratio (length/radius) of the interconnecting throat-like capillaries. The detailed definition of this optimal aspect ratio as a function of capillary length is given for a numerical surface generated from a range of capillary lengths and radii. For minimal filling time within a given feature of a network structure, this optimal aspect ratio was found to be approximately 0.5 for fluids similar to water entering a network structure containing fine-scale features of length < ~ 0.1 µm. Deviations of this optimum aspect ratio from 0.5 occur for both very long and/or very large radius capillary features, such that the optimum pathway effect by inertial selectivity is progressively lost as features become macroscopic, thus reverting to Lucas-Washburn, and the selected pathway then involves the larger radii

pores. Fluid properties affect the inertial selection of pores taking part in the observed preferred micro-pathway, with increasing density lengthening the time taken for filling along the same pathway and increasing viscosity creating a deviation of optimal aspect ratio making up the path to smaller values on account of the viscous drag in longer and finer capillaries.

REFERENCES

1. Bosanquet, C. H., *Phil. Mag. Series 6,* **45,** 525 (1923).

2. Szekely, J., Neumann, A. W., and Chuang, Y. K., *J. Colloid Interface Sci.,* **35,** 273 (1971).

3. Sorbie, K. S., Wu, Y. Z., and McDougall, S. R., *J. Colloid Interface Sci.,* 289 (1995).

4. Taylor, S. C., Hall, Ch., Hoff, W. D., and Wilson, M. A., *J. Colloid Interface Sci.,* 351 (2000).

5. Einset, E. O., *J. Am. Ceram. Soc.,* **79,** 333 (1996).

6. Yang, Y.-W., Zografi, G., and Miller, E. E., *J. Colloid Interface Sci.,* **122,** 35 (1988).

7. Van Oss, C. J., Giese, R. F., Li, Z., Murphy, K., Norris, J., Chaudhury, M. K., and Good, R. J., *J. Adhes. Sci. Technol.,* 413 (1992).

8. Dube, M., Rost, M., and Alava, M., *Eur. Phys. J. B,* **15,** 691 (2000).

9. Quere, D., *Europhys. Lett.,* **39,** 533 (1997).

10. Li, Z., Giese, R. F., Van Oss, C. J., Kerch, H. M., and Burdette, H. E., *J. Am. Ceram. Soc.,* **77,** 2220 (1994).

11. Fisher, L. R. and Lark, P. D., *J. Colloid Interface Sci.,* **69,** 486 (1979).

12. Chibowski, E. and Holysz, L., *J. Adhes. Sci. Technol.,* 1289 (1997).

13. Gane, P. A. C., Schoelkopf, J., Spielmann, D. C., Matthews, G. P., and Ridgway, C. J., *Tappi J.,* **83,** 77 (2000).

14. Schoelkopf, J., Ridgway, C. J., Gane, P. A. C., Matthews, G. P., and Spielmann, D. C., *J. Colloid Interface Sci.,* **227,** 119 (2000).

15. Schoelkopf, J., Gane, P. A. C., Ridgway, C. J., and Matthews, G. P., *Nord. Pulp Paper Res.,* **15,** 422 (2000).

16. Levine, S., Reed, P., Watson, E. J., and Neale, G. (1976), A theory of the rate of rise of a liquid in a capillary, Academic Press, New York.

17. Letelier, M. F. and Leutheusser, H. J., *J. Colloid Interface Sci.,* **72,** 465 (1979).

18. Batten, G. L., *J. Colloid Interface Sci.,* **102,** 513 (1984).

19. Ichikawa, N. and Satoda, Y., *J. Colloid Interface Sci.,* **162,** 350 (1994).

20. Marmur, A. and Cohen, R. D., *J. Colloid Interface Sci.,* **189,** 299 (1997).

21. Martic, G., Gentner, F., Seveno, D., Coulon, D., and DeConinck, J., *6th International Symposium on Evaluation of Reservoir Wettability and Its Effect on Oil Recovery, Soccoro, Mexico,* (2000).

22. Bell, J. M. and Cameron, F. K., *J. Phys. Chem.,* **10,** 658 (1906).

23. Kent, H. J., Climpson, N. A., Coggon, L., Hooper, J., and Gane, P. A. C., *Tappi J.,* **69,** 78 (1986).

24. Lucas, R., *Kolloid Z.,* **23,** 15 (1918).

25. Washburn, E. W., *Phys. Rev.,* **17,** 273 (1921).

26. Rideal, E. K., *Phil. Mag.,* 1152 (1922).

27. Wingrave, J.A., Wade, W.H. and Schechter, R.S. *S.C.I. Symposium,* Sept 1976, Loughborough, Academic Press, London, 261 (1978).

28. Levine, S., Lowndes, J., Watson, E. J., and Neale, G., *J. Colloid Interface Sci.,* **73,** 136 (1980).

29. LeGrand, E. J. and Rense, W. A., *J. Appl. Phys.,* **16,** 843 (1945).

30. Moshinskii, A. I., *Colloid J.,* **59,** 62 (1997).

31. Ridgway, C. J., Schoelkopf, J., Matthews, G. P., Gane, P. A. C., and James, P. W., *J. Colloid Interface Sci.,* **239,** 417 (2001).

32. Chatzis, I. and Dullien, F. A. L., *J. Colloid Interface Sci.,* **91,** 199 (1983).

33. O' Carroll, C. and Sorbie, K. S., *Phys. Rev. E,* **47,** 3467 (1993).

34. McDougall, S. R. and Sorbie, K. S., *Petrol. Geosci.,* **3,** 161 (1997).

35. Matthews, G. P., Moss, A. K., Spearing, M. C., and Voland, F., *Powder Technol.,* **76,** 95 (1993).

36. Ridgway, C. J., Ridgway, K., and Matthews, G. P., *J. Pharm. Pharmacol.,* **49,** 377 (1997).

37. Peat, D. M. W., Matthews, G. P., Worsfold, P. J., and Jarvis, S. C., *Eur. J. Soil Science,* **51,** 65 (2000).

38. Gane, P. A. C., Kettle, J. P., Matthews, G. P., and Ridgway, C. J., *Ind. Eng. Chem. Res.,* **35,** 1753 (1996).

39. Matthews, G. P., Ridgway, C. J., and Spearing, M. C., *J. Colloid Interface Sci.*, **171,** 8 (1995).

40. Engstrom, G., Norrdahl, P., and Ström, G., *Proc. Tappi Coating Conference*, 35, (1987).

41. Ridgway, C. J. and Gane, P. A. C., *TRI/Princeton International Workshop, Princeton*, (2001).

42. Gane, P. A. C. and Seyler, E. N., *Tappi Coating Conference Proceedings*, (1994).